Journal of Nuclear Medicine, published on December 16, 2021 as doi:10.2967/jnumed.121.263175

Radiation Protection and Occupational Exposure on [^{68}Ga]Ga-PSMA-11 based Cerenkov Luminescence Imaging Procedures in robot assisted Prostatectomy

Running Title: ^{68}Ga-PSMA CLI exposure in Prostatectomy

Pedro Fragoso Costa[1, 2], Wolfgang P. Fendler[1, 2], Ken Herrmann[1, 2], Patrick Sandach[1, 2], Hong Grafe[1,2], Maarten R. Grootendorst[3], Lukas Püllen[2, 4], Claudia Kesch[2, 4], Ulrich Krafft[2, 4], Jan P. Radtke[2, 4], Stephan Tschirdewahn[2, 4], Boris A. Hadaschik[2, 4] Christopher Darr[2, 4]

[1] Department of Nuclear Medicine, University Hospital Essen, Essen, Germany

[2] German Cancer Consortium (DKTK)-University Hospital Essen, Essen, Germany

[3] Clinical Department, Lightpoint Medical Ltd., Chesham, United Kingdom

[4] Department of Urology and Urological Oncology, University Hospital Essen, Essen, Germany

Contact information first author:

Pedro Fragoso Costa

Department of Nuclear Medicine, University Hospital Essen

Hufelandstraße 55

D-45147 Essen

Germany

Fax: + 49-201-723-5964

Phone: + 49-201-723-85010

email: pedro.fragoso-costa@uni-duisburg-essen.de

Corresponding authors:
Pedro Fragoso Costa
Department of Nuclear Medicine, University Hospital Essen
Hufelandstraße 55
D-45147 Essen
Germany
Fax: + 49-201-723-5964
Phone: + 49-201-723-85010
email: pedro.fragoso-costa@uni-duisburg-essen.de

Christopher Darr
Department of Urology and Urological Oncology, University Hospital Essen
Hufelandstraße 55
D-45147 Essen
Germany
email: christopher.darr@uk-essen.de

ABSTRACT

Introduction: Cerenkov Luminescence Imaging (CLI) was successfully implemented in the intraoperative context as a form of cancer radio-guided surgery, showing promise in the detection of surgical margins during robot-assisted radical prostatectomy (RARP). The current study was designed to provide a quantitative description on the occupational radiation exposure to surgery and histopathology personnel from CLI-guided RARP after injection of [^{68}Ga]Ga-PSMA-11 using a single injection PET/CT / CLI protocol.

Methods: Ten patients with preoperative [^{68}Ga]Ga-PSMA-11 administration and intraoperative CLI were included. Patient dose rate was measured, pre-PET/CT (N = 10) and post-PET/CT (N = 5) at one meter distance of four patient regions (A: head, B: right side, C: left side and D: feet). Electronic Personal Dosimeters (EPD) were used for intraoperative occupational exposure (N = 10). Measurements included the first surgical assistant and scrub nurse at the operating table and the CLI imager / surgeon at the robotic console, encompassing the whole duration of surgery and CLI image acquisition. An estimation of exposure to histopathology personnel was performed by measuring prostate specimens (N = 8) on a Germanium detector.

Results: The pre-PET/CT measured dose rate values averaged (± SD) 5.3 ± 0.9 µSv/h. This corresponds to a patient-specific dose rate constant for positions B and C of 0.047 µSv/h*MBq. Post PET/CT dose rate values averaged (± SD) 1.04 ± 1.00 µSv/h. The patient-specific dose rate constant values were 0.011 µSv/h*MBq, 0.026 µSv/h*MBq, 0.024 µSv/h*MBq and 0.003 µSv/h*MBq, corresponding to regions A-D. EPD readings revealed an average (±SD) personal equivalent dose of 9.0 ± 7.1, 3.3 ± 3.9, 0.7 ± 0.7 µSv for first surgical assistant, scrub nurse and CLI imager / surgeon, respectively. The median

(Interquartile range - IQR) Germanium detector measured activity of the prostate specimen was 2.96 kBq (2.23; 7.65 kBq).

Conclusion: Single injection of [^{68}Ga]Ga-PSMA-11 PET/CT / CLI procedures are associated with a reasonable occupational exposure level, if kept under 110 procedures per year. Excised prostate specimen radionuclide content was below the exemption level for Gallium-68. Dose rate based calculations provide a robust estimation for EPD measurements.

Key Words. *Cerenkov luminescence imaging; radioguided surgery; prostate cancer; margin assessment; radical prostatectomy*

INTRODUCTION

In men with local prostate cancer (PC) surgery or radiotherapy are the treatment modalities of choice. Radical prostatectomy (RP) with complete removal of the prostate and the PC aims to cure the patient, but collateral damage such as impotence and incontinence may occur. These greatly impair the quality of life, so that in the context of RP, the anatomical structures for continence and potency should be spared as much as possible (*1*) .In this regard, positive resection margins (PSM) may occur in nerve-sparing RP or in locally advanced PC. Martini et al. recently showed that the presence of PSM is associated with an increased risk of biochemical recurrence. In addition, the risk of metastasis is increased with PSM > 2 mm or multiple PSMs Preoperative MRI and prostate sampling with systematic and fusion-guided biopsy cores help to guide neurovascular bundle preservation planning without increasing the risk and number of PSMs (*2-4*). Intraoperative frozen section analysis (IFS) can help the surgeon to preserve these structures (*1,5*). However, besides resource consumption, there is also some conflicting evidence, as studies demonstrated high false-negative rates of IFS, potentially resulting in unjustified nerve-sparing surgery (*5,6*).

For PC, molecular imaging with radiopharmaceuticals targeting prostate specific membrane antigen (PSMA)-PET/CT has been established in recent years. PSMA-PET/CT is used for highly specific oncologic diagnostic imaging, especially in the setting of biochemical recurrence (*7-11*). Interestingly, PET imaging agents also emit optical photons via a phenomenon called Cerenkov luminescence. This enables optical imaging called Cerenkov Luminescence Imaging (CLI) using the novel LightPath system (Lightpoint Medical, Ltd, Chesham, United Kingdom) (*12*). Cerenkov photons are emitted

by a charged particle (e.g. positron or electron) when travelling through a dielectric medium at a faster speed than the velocity of light in that medium (*12,13*). Although Cerenkov luminescence has a broad wavelength spectrum, it predominantly comprises ultraviolet and blue light. These short wavelengths are highly attenuated in biological tissue. Therefore, CLI is limited to detection of signals emitted in superficial tissue layers. In contrast to PET, CLI is unable to detect photons emitted by deeper located tissues or tumors (*14,15*). Intraoperative imaging with CLI is promising since it allows to evaluate the entire surface of the prostate while IFS only analyses limited number of prostatic slices and thus is susceptible to sampling errors. Initial feasibility studies for intraoperative use in PC show promising results. So far, these are based on small patient cohorts and selected patients, mainly with intermediate to high risk PC. One difference between the studies is the number of injections. In Olde Heuvel et al. a preoperative PET/CT was performed 4 weeks prior to surgery with intraoperative tracer injection, whereas Darr et al. examined an immediate preoperative PET/CT without intraoperative tracer injection (*16,17*).

CLI could significantly improve the oncological outcome of this patient group in the future, however, the safety of the medical staff must also be guaranteed and ensured. Radiation exposure has been thoroughly evaluated for Sentinel Lymph Node procedures with ^{99m}Tc-labelled compounds, showing consistent values of exposure from 1-10 µSv (*18-21*) per procedure. However, PET tracers carry an inherent risk of additional radiation exposure due to the higher energy and number of annihilation gamma photons in comparison to the gamma photons from ^{99m}Tc (*22*). Olde Heuvel et al. presented first data with a maximum radiation exposure of 0.016 mSv per procedure as radiation exposure to

medical personnel in 5 patients undergoing CLI-guided RP after intraoperative [^{68}Ga]Ga-PSMA-11 administration (*17*).

To calculate a possible scenario for radiation exposure in a new situation, such as radio-guided surgery using positron emitters, medical physicists must rely on evidence-based publications. However, these are mostly available in a different situation, such as the clinical technologist exposure from patients undergoing PET/CT imaging or metrological data which is either theoretically determined or measured in very controlled situations, not corresponding a realistic clinical operation (*23,24*). Exposure limits must be observed and, if necessary, the operation theatre must be reclassified as a temporary radiation-controlled area.

The objective of this study was to provide a quantitative description of the total additional occupational exposure that would occur for surgery personnel and pathologists, from patients undergoing preoperative ^{68}Ga-PSMA-PET/CT and subsequent radio-guided radical prostatectomy (RARP).

MATERIALS AND METHODS

Surgery and Intraoperative CLI

Ten patients with preoperative [^{68}Ga]Ga-PSMA-11 administration and intraoperative CLI were included in the present radiation exposure study (five of which were investigated for post-PET/CT gamma field dose rate). The workflow of our one-stop-shop protocol is shown in Figure 1. Patients received an average ± SD of 141.9 ± 57.86 MBq [^{68}Ga]Ga-PSMA-11 for PET/CT, following guideline recommendations (*25*). After ^{68}Ga-PSMA-PET/CT, robot-assisted RP was performed. A urinary catheter was inserted in the operating room to drain the urine. The excised prostate specimen was immediately retrieved from the abdomen, wiped to clear blood and fluids, positioned in a specimen tray and then imaged in the LightPath system. After accomplishing the imaging, the prostate gland was assessed for radioactivity quantification in a Germanium detector.

Patient Dose Rate

An initial evaluation of the detector response consisted of three measurements of a point source of 60 MBq, using a proportional-counter based dose rate meter FH 40 G-L (Thermo Fisher Scientific, Waltham, MA, United States), all measurements include background subtraction.

Subsequently, we evaluated the impact of the patient orientation towards the radiation detector, compared with a point source, and later provided a rough estimation of the fraction of tracer elimination until prostatectomy. For this, we measured 10 patients injected with [^{68}Ga]Ga-PSMA-11 (average ± SD; 10.4 ± 4.6 min post injection), in standing position facing the right and left side of the waist, with the condition that the patient did not eliminate any tracer via urine excretion (pre-PET/CT). Following (average ± SD; 100.2 ±

27.5 min post injection) [^{68}Ga]Ga-PSMA-11 PET/CT scanning, measurements were performed in five patients in supine position (post-PET/CT). In total four predefined positions were measured (coded as: A – head, B – right side of the waist, C – left side of the waist, D – feet) at a distance of one meter. These predefined positions correspond to the locations around the patient where staff members (e.g. scrub nurse, surgical assistant) are likely to be stationary positioned during surgery including CLI. In total, 20 individual measurements were performed.

The measured dose rates were plotted as a function of the injected tracer activity decay-corrected to the time of measurement and a linear fit (least square method) was applied, constraining the fit to pass at the origin (i.e. the condition in which there is no tracer, the dose rate output will be equal to that measured as background signal). We postulate that the slope of the fit provides an estimate for the patient-specific dose rate constant at the defined positions.

Electronic Personal Dosimetry (EPD)

Exposure to the medical personnel were assessed in ten procedures using electronic personal dosimeters (EPD). In this study, RAD-60 (Mirion Technologies, San Ramon, CA, US) EPD's were positioned at waist level. Measurements included the first surgical assistant, scrub nurse at the operating table and the CLI imager / surgeon at the robotic console encompassing the whole duration of surgery.

EPD vs dose rate predictions

Based on the different patient-specific dose rate constants at the defined positions, the exposure during the procedure is calculated as:

$$H^*(10) = \frac{\Gamma_{H^*} \cdot A}{r^2} \cdot RF \qquad \text{Equation (1)}$$

, where $\dot{H}^*(10)$ is the personal dose equivalent at 10 mm depth, A the radionuclide activity and r the distance from source to detector. Since Gallium-68 is a short-lived radionuclide (half-life value of 67.71 min), the activity present in a given sample will decrease as a function of the time of measurement, which causes a decrease in the dose rate. Taking this phenomenon into account, we introduce a correction factor that is obtained by integrating the dose rate over the measured time (t); this factor is referred as reduction factor (*24*):

$$RF = 1.433 \cdot \frac{T_{1/2}}{t} \cdot \left(1 - exp[\frac{0.693 \cdot t}{T_{1/2}}]\right) \qquad \text{Equation (2)}$$

Since in robot-assisted surgery, the operating room personnel is mostly stationary, it is reasonable to assume that the point source exposure modelling will provide a reasonable estimation. If we measure the typical distance from the source to the exposed professional (Figure 2), we obtain that r is equal to 0.3 m, 0.6 m and 1 m, corresponding to the first assistant, scrub nurse and the CLI imager (which is also a conservative surrogate for the anaesthetist and the primary surgeon at the console). To accommodate any uncertainty related to the exact position of each health professional, two additional points on ± 10 cm of the reference positions were considered. The health professional positions were then superimposed on Figure 3, such that the first surgical assistant and the CLI imager / surgeon were attributed the dose rate value corresponding to point C, while the scrub nurse that one calculated from point B.

Prostate Gland Specimen

To access the tracer activity present in the prostate gland, as an indicator for pathologist's skin exposure, eight prostate specimens were measured in a Hyper-Pure

Germanium detector (HPGe) (Canberra, Meridon, CT, USA), after prostate excision and CLI. To ensure adequate pathological processing afterwards, the specimens were already placed in formalin. The radiation measurement was performed using a 20-min protocol, followed by an automatic sequence for the identification of the 511 keV energy peak and further quantification based on energy and efficiency calibration curves.

The detected activity at the HPGe provides an exposure estimate to the pathologists that perform frozen section procedures. As a threshold, we use the nuclide-specific exemption limits (Gallium-68 < 100 kBq) (*26*).

Because not all centres may have access to HPGe detectors, we present an alternative method for accessing the amount of radiotracer present at the excised specimen based on [^{68}Ga]Ga-PSMA-11 imaging. The method consists in defining a region delimited by the prostate anatomical boundaries, based on CT imaging. The same volume is then overlaid to the PET reconstructed images, as to provide an estimate of the total amount of tracer.

RESULTS

Patient Dose Rate

Initial measurements around the patient, show a decreased dose rate constant when compared with a point source. The measured dose rate values averaged 5.3 ± 0.9 µSv/h. If we assume a linear relationship between the dose rate and tracer activity (decay corrected to the time of measurement), we can extract the patient-specific dose rate constant for each measured position, showing both B (n=10) and C positions (n=10) 0.047 µSv/h*MBq vs 0.145 ± 0.002 µSv/h*MBq for the point source (Table 1).

The dose rate measurements immediately prior to surgery (post-PET/CT) averaged 1.04 ± 1.00 µSv/h (minimum 0.115 µSv/h, maximum 3.65 µSv/h). Lowest dose rates were detected at the head and the feet of the patients. The patient-specific dose rate constant value obtained from a linear modulation, showed 0.011 µSv/h*MBq, 0.026 µSv/h*MBq, 0.024 µSv/h*MBq and 0.003 µSv/h*MBq, corresponding to the regions head (A), right waist (B), left waist (C) and feet (D).

Patient Demographics and Oncological Data

Patient characteristics are displayed in Table 2. In total 10 patients with histologically confirmed PC were included, among those 50% with a locally advanced disease and 50% with a high-risk PC. Median (Interquartile range – IQR) time from tracer injection until CLI was 328.5 min (298.75 min; 371.75 min). This study received formal Ethical Committee approval (19-8749-BO) and all subjects signed a written informed consent.

EPD

For the 10 procedures considered, EPD monitoring duration was in average (±SD) for 242 ± 14 min, starting 189 ± 38 min after [^{68}Ga]Ga-PSMA-11 administration. EPD readings revealed an average (±SD) personal equivalent dose – Hp(10) – of 9.0 ± 7.1, 3.3 ± 3.9, 0.7 ± 0.7 µSv for first surgical assistant, scrub nurse and the CLI imager / surgeon at the robotic console, respectively.

EPD vs Dose Rate Predictions

Regarding the calculated personal equivalent dose based on patient-specific dose rate constants, we observe an average Hp(10) (±SD) of 11.7 ± 10.0, 2.7 ± 1.7, 0.8 ± 0.5 µSv for first surgical assistant, scrub nurse and CLI imager / surgeon, respectively. This corresponds to a success rate (condition in which the read EPD value falls within the ± 10 cm uncertainty calculated exposure) of 90%, 40% and 20% for first surgical assistant, scrub nurse and CLI imager / surgeon, respectively. The procedure-specific values of exposure can be consulted in Figure 4.

Prostate Gland Specimen

Prostate gland specimens were excised and analysed in the CL-imager in median 348 min (IQR: 282; 437 min) after [^{68}Ga]Ga-PSMA-11 administration and 276 min (IQR: 194; 369 min) after PET/CT imaging. The measurements in the HPGe were performed 71 min (IQR: 42; 143 min) after prostate excision. All activity values were decay-corrected to the time of prostate excision.

HPGe Measurements revealed activities between 0.9 and 38.6 kBq for Gallium-68. The median HPGe measured activity was 2.96 kBq (IQR: 2.23; 7.65 kBq), while the

median total activity encompassed in the prostate region PET reconstructed images accounted for 3.83 kBq (IQR: 2.83; 8.50 kBq).

The deviation between HPGe and PET activity values was characterised by a systematic overestimation (median of 18.9%) of PET activity values when compared to HPGe as depicted in Figure 5. There were no statistical differences between HPGe and PET datasets regarding the prostate activity levels ($p = 0.090$).

DISCUSSION

In this study, we were able to provide a systematic evaluation of the patient as radioactive source in each of the different procedural steps encountered in PET/CT imaging and thereafter CLI for the evaluation of surgical margins during robot assisted prostatectomy, for a single administration protocol (i.e. one-stop-shop protocol, Figure 1). For this purpose, methods for prospective and department planning radiation protection calculations for this entirely new application of [^{68}Ga]Ga-PSMA-11 were used, including the point source exposure calculation and a reduction factor expected for long exposures to short-lived radionuclides.

In the first step of this study, a measurement was elected to illustrate how the point source exhibits similar dose rate per unit activity at 1 meter distance. The resulting dose rate at one meter normalised for activity shows a good concordance with the DIN tabulated value of 0.1581 (0.145 measured) µSv • h^{-1} • MBq^{-1} for Gallium-68. The observed discrepancy is mainly due to a decreased detector responsivity to 511 keV, compared to the calibration gamma lines of Cs-137 (661.6 keV). However, for patients, partially due to self-attenuation (*27*), a discrepancy between tabulated values and those based on dose rate meter measurements is observed (Table 1). Furthermore, the fact that the dose rate meter is positioned at a 1 meter distance from a source that is greater than that distance in height, will deliver a lower dose rate from that one of a point source assumption (*28*). Dose rate measurements performed after the PET/CT scan show a decreased dose rate constant due to the fact that much of the tracer has been excreted at this point, leading to a decrease in dose rate constants roughly 50 % when compared to the values immediately after tracer injection (i.e. pre-PET/CT).

Despite being a simple and limited method, the point source approximation using patient-specific dose rate constants provided a plausible approximation for the occupational exposure measured by EPDs. Especially considering the position of the assistant surgeon, in which a relaxation of ± 10 cm to the stationary condition could predict 90 % of the measured doses. The greatest impairment on the dose estimation was due to very low exposure levels, illustrated by the CLI Imager / Surgeon position in which most values of exposure were found to be between 0 and 1 µSv, suggesting that the limiting factor is the EPD lack of accuracy for measurements below the measuring range (1 µSv – 9.99 Sv). The remainder of outliers could be explained due to a higher proximity to the source or orientation of the dosimeter towards the radiation field outside the efficient angular range of the EPD.

With respect to the measured Hp(10), it is evident from Equation (2) that the professional that operated nearest to the patient will have a highest exposure. Considering the general public exposure limit of 1 mSv as a threshold, that professional of highest exposure, first surgical assistant (Figure 4A), would be able to perform CLI imaging post [^{68}Ga]Ga-PSMA-11 PET/CT on 110 RARP procedures per year.

The presented “one-stop-shop” single administration for both PET/CT and CLI has been validated in a feasibility study (*16*) and displays an example of the ALARA principle (As Low As Reasonably Achievable) for radiation exposure optimisation applied to radio-guided surgery. Not only for the patient medical exposure, by relinquishing a dedicated tracer injection of about 100 MBq, which results on a patient effective dose of 2 mSv, but also effectively decreasing the occupational exposure for the medical personnel. In a [^{68}Ga]Ga-PSMA-11 CLI primary prostate cancer study (*16*), performing perioperative radiotracer administration of 100 MBq, a Hp(10) of 16 µSv was recorded for the most

exposed medical professional. The data presented are for the sterile scrub nurse and are comparable to our collected data. However, no other exposure data were collected from other staff roles. According to our findings, the exposure values for the scrub nurse are quite variable (average ± SD Hp(10) equal to 3.3 ± 3.9 μSv), whereas the exposure of the assistant is very precise and therefore more informative.

Other intraoperative CLI applications include the use of 2-[^{18}F]FDG for the identification of surgical margins in breast conserving surgery. From published studies, there is evidence that a pre-operative administration of about 300 MBq of 2-[^{18}F]FDG would deliver maximal personal equivalent doses of 34.0 – 61.8 μSv (*14,29*). Interestingly, if the Fluorine-18 decay characteristics and assuming an administration of 300 MBq are substituted in our model, we obtain exposure levels of 51.3, 15.3 and 4.6 μSv per procedure for the first surgical assistant, scrub nurse and robotic surgeon, respectively.

CLI has been foremost important in pre-clinical evaluations of disease models using a number of beta-emitters, mostly due to the small dimensions of the images samples (mostly mice), which are favourable for CLI, and the cost-efficiency compared to pre-clinical PET/CT scanners. With the translation in the intraoperative environment it is conceivable that new radionuclides will become relevant in radioguided surgery by CLI (such as the longer lived ^{89}Zr or ^{64}Cu), for which our exposure model could provide some insight in terms of predicting occupational exposures (*30*).

Our approach for the pathologist's exposure, was a conservative surrogate for a direct measurement of exposure with a ring dosimeter, by directly measuring the activity contained in the prostate gland using the HPGe. Based on our data, there is no significant radiation exposure to pathology staff. Additionally, an independent measurement is provided based on PET data performed prior to CLI. Our results indicate a systematic

overestimation of the activity levels found by PET in comparison with the HPGe. The systematic result suggests that this method of tracer amount estimation may be limited by the presence of activity in surrounding tissues, namely the bladder, that would overestimate the radioactivity content in the prostate specimen. However, to the exception of one specimen, the PET estimate could predict the HPGe below 10% error. Various standardized exposure situations are given in the literature. Delacroix et al describe hand contact to a glass beaker filled with 50 mL of Gallium-68 solution (*26*). With this method, a dose of approximately 4 µSv would be expected from a one-hour contact. This specification is consistent with our results, considering the 50 mSv radiation exposure limit to the skin for members of the public (*31*).

Our study inherits several limitations. First, our study is related to the low radiation field that provides poor statistics for the counting devices. This also translates in the difficulty for the point source model to predict such low exposures. Secondly, the fact that we use a point source geometry is also a limitation, as in real life the patient is not a point source. Further studies using anthropomorphic mathematical phantoms as the source of external exposure could tackle this limitation (*32*). Finally, we do not provide a measured evidence of the skin exposure, by means of a ring dosimeter, and therefore cannot directly correlate the activity levels in the specimen to the finger exposure of histopathology staff.

CONCLUSION

The presented single injection PET/CT / CLI-guided RARP protocol can be performed about 110 procedures per year before reaching the limit for public radiation exposure. All prostate specimen radionuclide content was below the exemption level for Gallium-68, at the time of excision. Overall, the occupational risk of the one-stop-shop protocol appears to be quite low, meaning that it is not necessary to reclassify the operation theatre as a temporary radiation-controlled area. Furthermore, no radiation safety measures are required for specimen handling in the pathology department. Further validation for other radionuclides with potential for CLI or other radioguided surgery, such as ^{18}F-PSMA-1007, should be addressed in future studies.

DISCLOSURE

Wolfgang P. Fendler reports fees from BTG (consultant), Calyx (consultant), RadioMedix (PET reader), Bayer (speakers bureau), and Parexel (image reader) outside of the submitted work.

K. Herrmann reports personal fees from Bayer, personal fees and other from Sofie Biosciences, personal fees from SIRTEX, non-financial support from ABX, personal fees from Adacap, personal fees from Curium, personal fees from Endocyte, grants and personal fees from BTG, personal fees from IPSEN, personal fees from Siemens Healthineers, personal fees from GE Healthcare, personal fees from Amgen, personal fees from Novartis, personal fees from ymabs, personal fees from Aktis Oncology, personal fees from Theragnostics, personal fees from Pharma15, outside the submitted work. KH is an associate editor of the JNM.

M Grootendorst is an employee of Lightpoint Medical Ltd.

B. Hadaschik has had advisory roles for ABX, Astellas, AstraZeneca, Bayer, Bristol Myers Squibb, Janssen R&D, Lightpoint Medical, Inc., and Pfizer; has received research funding from Astellas, Bristol Myers Squibb, German Research Foundation, Janssen R&D, and Pfizer; and has received compensation for travel from Astellas, AstraZeneca, and Janssen R&D.

The other authors declare that no relevant conflict of interest relevant to this article exist.

ACKNOWLEDGEMENTS

The authors would like to thank technologists of the nuclear medicine and nurses of the urology surgery teams for their ongoing logistic support.

KEY POINTS

QUESTION: What is the radiation exposure risk for CLI radioguided surgery after [^{68}Ga]Ga-PSMA-11 administration for surgery personnel?

PERTINENT FINDINGS: The protocol can be performed about 110 procedures per year before reaching the limit for public radiation exposure.

IMPLICATIONS FOR PATIENT CARE: Implementation of CLI radioguided surgery procedures do not require additional radioprotection hurdles.

REFERENCES

1. EAU Guidelines. Edn. presented at the EAU Annual Congress Milan 2021. ISBN 978-94-92671-13-4.

2. Gandaglia G, Ploussard G, Valerio M, et al. The key combined value of multiparametric magnetic resonance imaging, and magnetic resonance imaging–targeted and concomitant systematic biopsies for the prediction of adverse pathological features in prostate cancer patients undergoing radical prostatectomy. *European urology.* 2020;77:733-741.

3. Radtke JP, Hadaschik BA, Wolf MB, et al. The impact of magnetic resonance imaging on prediction of extraprostatic extension and prostatectomy outcome in patients with low-, intermediate-and high-risk prostate cancer: try to find a standard. *J Endourol.* 2015;29:1396-1405.

4. Petralia G, Musi G, Padhani AR, et al. Robot-assisted radical prostatectomy: multiparametric MR imaging–directed intraoperative frozen-section analysis to reduce the rate of positive surgical margins. *Radiology.* 2015;274:434-444.

5. Schlomm T, Tennstedt P, Huxhold C, et al. Neurovascular structure-adjacent frozen-section examination (NeuroSAFE) increases nerve-sparing frequency and reduces positive surgical margins in open and robot-assisted laparoscopic radical prostatectomy: experience after 11 069 consecutive patients. *European urology.* 2012;62:333-340.

6. Gillitzer R, Thüroff C, Fandel T, et al. Intraoperative peripheral frozen sections do not significantly affect prognosis after nerve-sparing radical prostatectomy for prostate cancer. *BJU international.* 2011;107:755-759.

7. Perera M, Papa N, Roberts M, et al. Gallium-68 prostate-specific membrane antigen positron emission tomography in advanced prostate cancer—updated diagnostic utility, sensitivity, specificity, and distribution of prostate-specific membrane antigen-avid lesions: a systematic review and meta-analysis. *European urology.* 2020;77:403-417.

8. Yaxley JW, Raveenthiran S, Nouhaud FX, et al. Risk of metastatic disease on 68gallium-prostate-specific membrane antigen positron emission

tomography/computed tomography scan for primary staging of 1253 men at the diagnosis of prostate cancer. *BJU international.* 2019;124:401-407.

9. Koschel S, Murphy DG, Hofman MS, Wong L-M. The role of prostate-specific membrane antigen PET/computed tomography in primary staging of prostate cancer. *Current opinion in urology.* 2019;29:569-577.

10. Kalapara AA, Nzenza T, Pan HYC, et al. Detection and localisation of primary prostate cancer using (68)gallium prostate-specific membrane antigen positron emission tomography/computed tomography compared with multiparametric magnetic resonance imaging and radical prostatectomy specimen pathology. *Bju International.* 2020;126:83-90.

11. Morris MJ, Carroll PR, Saperstein L, et al. Impact of PSMA-targeted imaging with 18F-DCFPyL-PET/CT on clinical management of patients (pts) with biochemically recurrent (BCR) prostate cancer (PCa): Results from a phase III, prospective, multicenter study (CONDOR). *Am J Clin Oncol.* 2020;38:5501-5501.

12. Das S, Thorek DL, Grimm J. Cerenkov imaging. *Advances in cancer research.* 2014;124:213-234.

13. Grootendorst MR, Cariati M, Kothari A, Tuch DS, Purushotham A. Cerenkov luminescence imaging (CLI) for image-guided cancer surgery. *Clin Transl Imaging.* 2016;4:353-366.

14. Grootendorst MR, Cariati M, Pinder SE, et al. Intraoperative Assessment of Tumor Resection Margins in Breast-Conserving Surgery Using (18)F-FDG Cerenkov Luminescence Imaging: A First-in-Human Feasibility Study. *J Nucl Med.* 2017;58:891-898.

15. Chin PT, Welling MM, Meskers SC, Olmos RAV, Tanke H, van Leeuwen FW. Optical imaging as an expansion of nuclear medicine: Cerenkov-based luminescence vs fluorescence-based luminescence. *European journal of nuclear medicine and molecular imaging.* 2013;40:1283-1291.

16. Darr C, Harke N, Radtke JP, et al. Intraoperative (68)Gallium-PSMA Cerenkov Luminescence Imaging for surgical margins in radical prostatectomy - a feasibility study. *J Nucl Med.* 2020;61:1500-1506.

17. Olde Heuvel J, van der Poel HG, Bekers EM, et al. 68 Ga-PSMA Cerenkov luminescence imaging in primary prostate cancer: first-in-man series. *European journal of nuclear medicine and molecular imaging.* 2020;47:2624-2632.

18. Bekiş R, Celik P, Uysal B, et al. Exposure of surgical staff to radiation during surgical probe applications in breast cancer. *Journal of Breast Cancer.* 2009;12:27-31.

19. Klausen T, Chakera A, Friis E, Rank F, Hesse B, Holm S. Radiation doses to staff involved in sentinel node operations for breast cancer. *Clinical physiology and functional imaging.* 2005;25:196-202.

20. Waddington W, Keshtgar M, Taylor I, Lakhani S, Short M, Eli P. Radiation safety of the sentinel lymph node technique in breast cancer. *European journal of nuclear medicine.* 2000;27:377-391.

21. Brenner W, Ostertag H, Peppert E, et al. Radiation exposure to the personnel in the operating room and in the pathology due to SLN detection with Tc-99m-nanocolloid in breast cancer patients. *Nuklearmedizin.* 2000;39:142-145.

22. Heckathorne E, Dimock C, Dahlbom M. Radiation dose to surgical staff from positron-emitter-based localization and radiosurgery of tumors. *Health physics.* 2008;95:220-226.

23. Costa PF, Reinhardt M, Poppe B. Occupational exposure from F-18-FDG PET/CT: implementation to routine clinical practice. *Radiation protection dosimetry.* 2018;179:291-298.

24. Madsen MT, Anderson JA, Halama JR, et al. AAPM task group 108: PET and PET/CT shielding requirements. *Medical physics.* 2006;33:4-15.

25. Fendler WP, Eiber M, Beheshti M, et al. 68 Ga-PSMA PET/CT: Joint EANM and SNMMI procedure guideline for prostate cancer imaging: version 1.0. *European journal of nuclear medicine and molecular imaging.* 2017;44:1014-1024.

26. Delacroix D, Guerre JP, Leblanc P, Hickman C. Radionuclide and radiation protection data handbook 2002. *Radiation protection dosimetry.* 2002;98:1-168.

27. Zeff BW, Yester MV. Patient self-attenuation and technologist dose in positron emission tomography. *Medical physics.* 2005;32:861-865.

28. Yi Y, Stabin M, McKaskle M, Shone M, Johnson A. Comparison of measured and calculated dose rates near nuclear medicine patients. *Health physics.* 2013;105:187-191.

29. Jurrius PA, Grootendorst MR, Krotewicz M, et al. Intraoperative [18 F] FDG flexible autoradiography for tumour margin assessment in breast-conserving surgery: a first-in-human multicentre feasibility study. *EJNMMI research.* 2021;11:1-12.

30. Collamati F, van Oosterom MN, Hadaschik BA, Darr C. Beta radioguided surgery: towards routine implementation? *The Quarterly Journal of Nuclear Medicine and Molecular Imaging: Official Publication of the Italian Association of Nuclear Medicine (AIMN)[and] the International Association of Radiopharmacology (IAR),[and] Section of the Society of.* 2021.

31. The 2007 Recommendations of the International Commission on Radiological Protection. ICRP publication 103. *Ann ICRP.* 2007;37:1-332.

32. Xu XG. An exponential growth of computational phantom research in radiation protection, imaging, and radiotherapy: a review of the fifty-year history. *Physics in Medicine & Biology.* 2014;59:R233–R302.

Figures and Tables

Figure 1

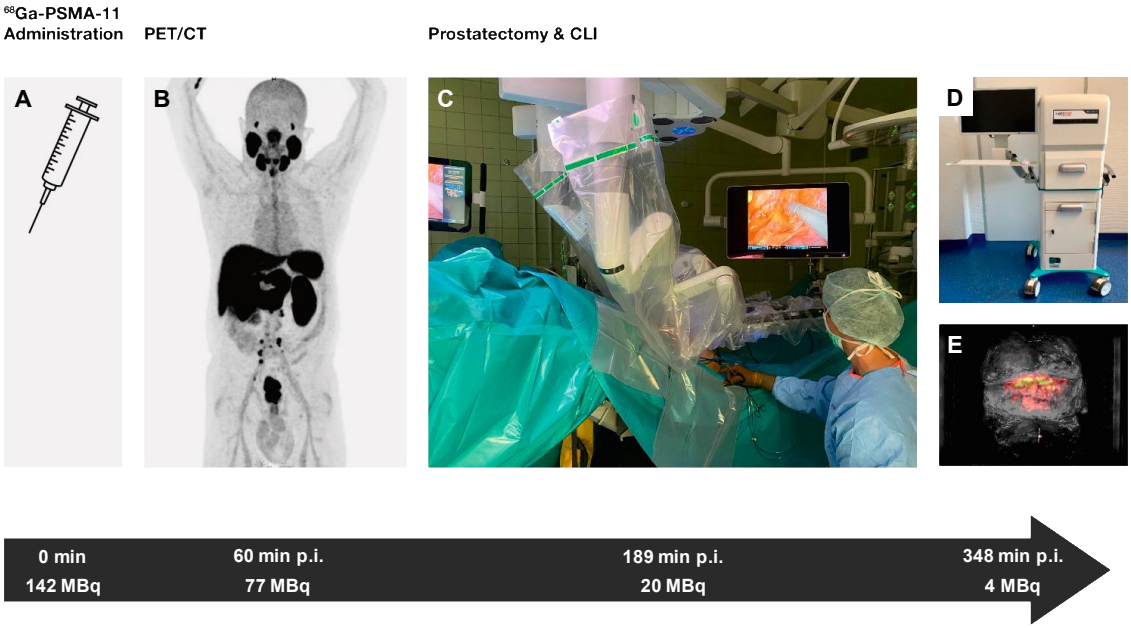

Figure 1 – One stop-shop-protocol, including tracer administration (A), PET/CT imaging (B) and CLI during prostatectomy (C-E), permitted by the remainder [^{68}Ga]Ga-PSMA-11 uptake in the prostate. The temporal sequence (black arrow) shows median time-points post injection (p.i.) and decay corrected whole body activity expected for each step of the protocol.

Figure 2

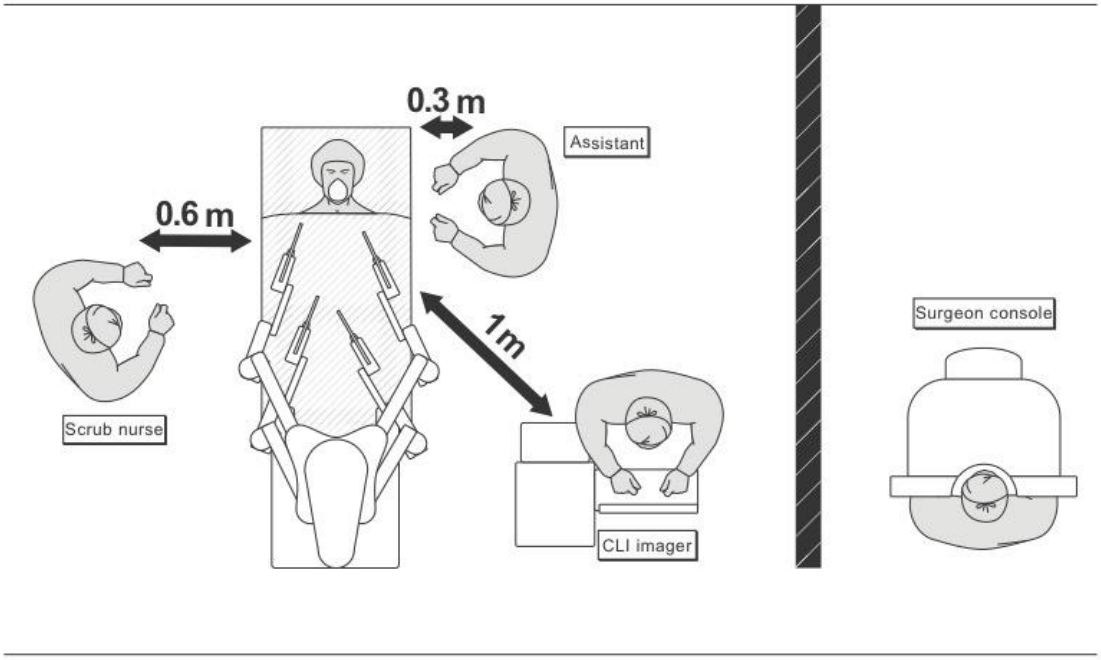

Figure 2 Set up in the operation theatre and respective distances used for calculated personal equivalent dose based on patient-specific dose rate constants.

Figure 3

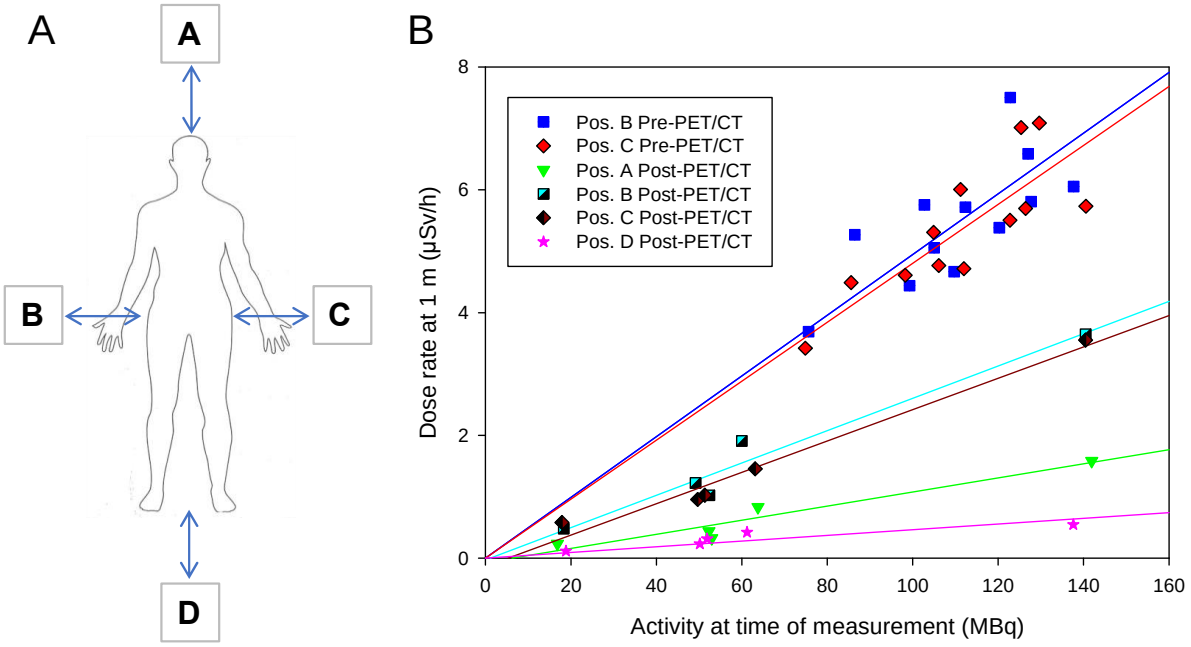

Figure 3 Dose rate measurements at the predefined positions (panel A) and the respective linear regression lines (panel B). Pre-PET refers to measurements immediately after tracer injection and Post-PET to dose rate readings immediately before entering the operation room. A: Position at the head, B: Position at the right side, C: Position at the left side, D: Position at the feet.

Figure 4

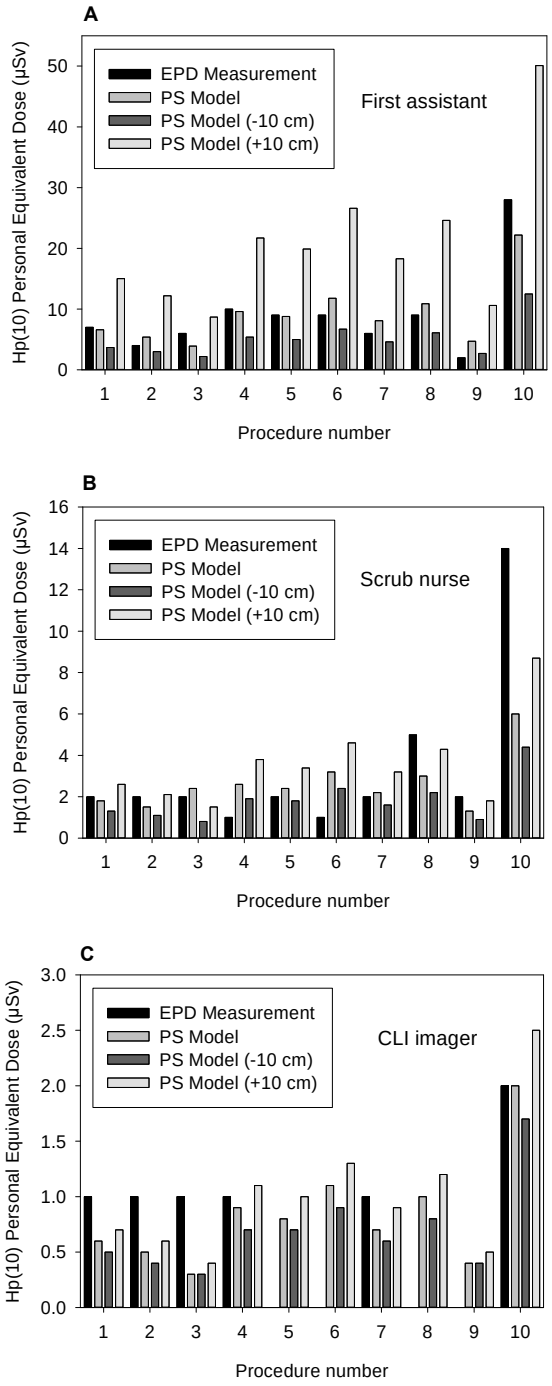

Figure 4 - EPD measurements (black bars) sided by the computed values based on a point source (PS) Model (medium gray bars) at the measured distance *r*. Variations of minus 10 cm (dark gray bars) and plus 10 cm (light bars) of the distance *r,* using a point source assumption.

Figure 5

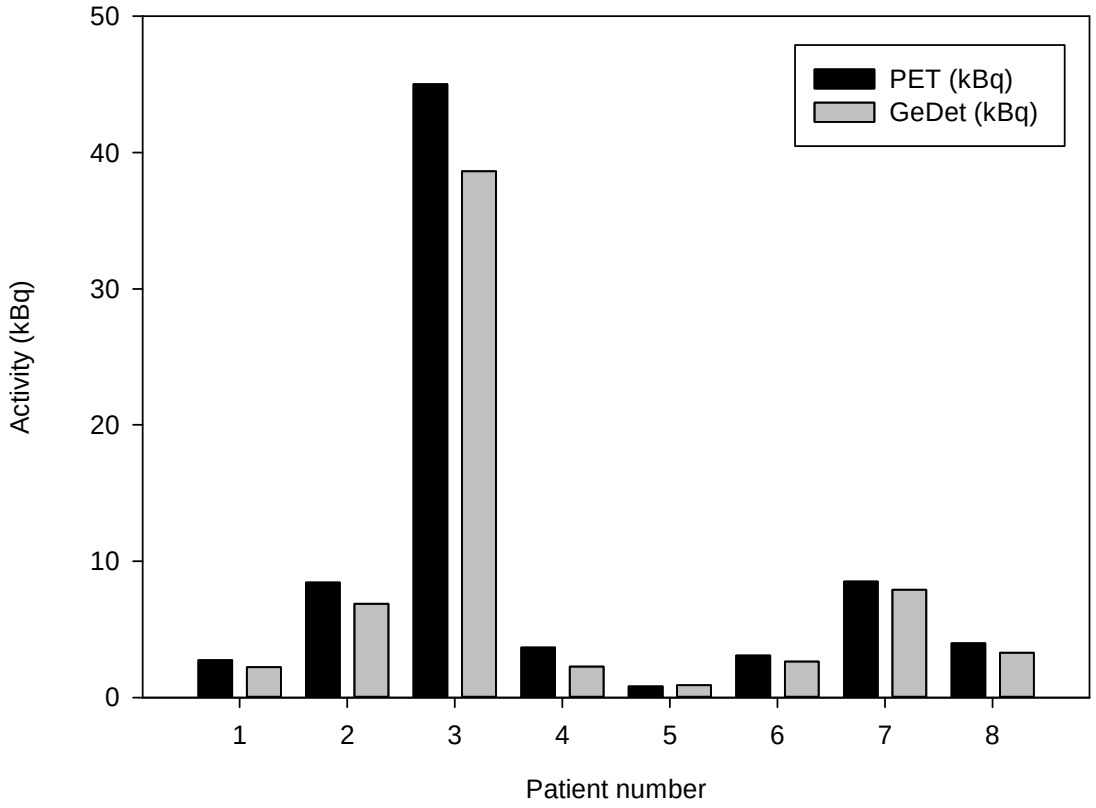

Figure 5 – Activity quantification of excised prostate specimens decay corrected to the time of excision. Black bars represent PET-based quantification (median: 3.83 kBq; IQR: 2.83; 8.50 kBq). Gray bars represent the HPGe measurement (median: 2.96 kBq; IQR: 2.23; 7.65 kBq).

Table 1

Table 1. Summary of performed dose rate measurements, activity at the time of measurement and respective patient-specific dose rate constants (Dose Rate / Activity)

Position	**Activity average ± SD (MBq)**	**Dose Rate / Activity average ± SD (μSv • h^{-1} • MBq^{-1})**
Point Source (1m)		
Centred at point	69.96 ± 2.3	0.145 ± 0.002
Patient Pre-PET (1m)		
B	112.2 ± 17.7	0.047 ± 0.004 (r^2 = 0.70)
C		0.047 ± 0.005 (r^2 = 0.66)
Patient Post-PET (1m)		
A	64.5 ± 41.7	0.011 ± 0.003 (r^2 = 0.92)
B		0.026 ± 0.004 (r^2 = 0.96)
C		0.024 ± 0.005 (r^2 = 0.97)
D		0.003 ± 0.004 (r^2 = 0.84)

Table 2

Table 2. Patient demographic and oncological data

Patient and imaging characteristics (N=10)	
Median age in years (IQR)	63 (56.5; 69)
Median BMI in kg/m^2 (IQR)	30.37 (24.25; 34.68)
Median injected activity in MBq (IQR)	122 (99.25; 185)
Median activity derived from HPGe in kBq/mL (IQR) – corrected to the time of excision	2.96 (2.24; 7.65)
Median activity derived from PET/CT in the prostate kBq/mL (IQR) – corrected to the time of excision	3.83 (2.83; 8.50)
Median duration from tracer injection to CLI (min)	328.5 (298.75; 371.75)
Median duration from skin incision to CLI in minutes (IQR)	130.2 (125.4; 145.2)
Surgical and oncological characteristics (N=10)	
Organ-confined PC (%)	5 (50%)
Locally-advanced PC (%)	5 (50%)
Initial PSA in ng/ml (IQR)	12.5 (8.3; 15.25)
Risk stratification according to D'Amico Intermediate risk PC (%) High risk PC (%)	 5 (50%) 5 (50%)
ISUP-GGG 2 3 4 5	 4 (40%) 4 (40%) 0 2 (20%)
Prostate specimen weight in g (IQR)	43.5 (41.25; 55)

BMI = Body-mass-index, CLI = Cerenkov luminescence imaging, IQR = Interquartile range, ISUP-GGG = International Society of Urological Pathology Gleason grading groups, PC = Prostate cancer, PSA = prostate specific antigen.

Graphical Abstract